J. Fluid Mech. (1982), *vol.* 116, *pp.* 91–114
Printed in Great Britain

The instability of oscillatory plane Poiseuille flow

By CHRISTIAN H. VON KERCZEK

Mechanical Engineering Department,
The Catholic University of America, Washington, D.C.

(Received 13 October 1980 and in revised form 28 April 1981)

The instability of oscillatory plane Poiseuille flow, in which the pressure gradient is time-periodically modulated, is investigated by a perturbation technique. The Floquet exponents (i.e. the complex growth rates of the disturbances to the oscillatory flow) are computed by series expansions, in powers of the oscillatory to steady flow velocity amplitude ratio, about the values of the growth rates of the disturbances of the steady flow. It is shown that the oscillatory flow is more stable than the steady flow for values of Reynolds number and disturbance wave number in the vicinity of the steady flow critical point and for values of frequencies of imposed oscillation greater than about one tenth of the frequency of the steady flow neutral disturbance. At very high and low values of imposed oscillation frequency, the unsteady flow is slightly less stable than the steady flow. These results hold for the values of the velocity amplitude ratio at least up to 0·25.

1. Introduction

The study of the instability characteristics of oscillatory plane Poiseuille (OPP) flow is of interest as a prototype problem in the class of time-periodic shear flows. This class of flow problems may have industrial applications as well as applications to the field of physiological fluid mechanics. A recent review of the stability theory of time-periodic flows was given by Davis (1976).

Oscillatory plane Poiseuille flow consists of the superposition of the steady parabolic axial flow velocity profile and an axial oscillatory velocity profile. The oscillatory velocity profile consists of Stokes layers at the channel walls matched to an oscillating slug flow in the core of the channel. The linear stability theory of this OPP flow has been examined by Grosch & Salwen (1968), Herbert (1972) and Hall (1975). These three studies contain certain conclusions concerning the stability characteristics of this flow that are not entirely in obvious accord.

The pioneering work of Grosch & Salwen (1968) used the Galerkin method and numerical time integration to compute the stability characteristics of OPP flow at some selected values of oscillation frequency and amplitude, disturbance wave-number α and mean Reynolds number R. Near the critical point, $\alpha = \alpha_c = 1{\cdot}0206$ and $R = R_c = 5772{\cdot}22$ of the underlying steady flow, Grosch & Salwen found that OPP flow seems to be more stable in the sense that the growth (decay) rate of the principal disturbance mode was smaller (larger) in the unsteady flow. This result holds, according to Grosch & Salwen, only for the values of the ratio of oscillation velocity amplitude to mean velocity amplitude that are less than about 0·105. For larger values of this ratio and at oscillation frequency that is equal to the principal

disturbance frequency, Grosch & Salwen find a rather drastic destabilization of the flow.

Herbert (1972) examined the disturbance energy transfer in the thin Stokes layers at the channel walls of OPP flow. He concluded that for small values of the oscillatory basic-state velocities the disturbance experiences a net decay in the wall region over one cycle of the oscillation if the oscillation frequency is greater than one-fourth the disturbance frequency. Herbert interpreted this to mean that the entire flow field is thus stabilized by the oscillations.

However, Hall (1975) finds that at very high frequency the oscillations may destabilize the mean flow at any value of the oscillation amplitude. The frequency of the imposed oscillations, for the validity of Hall's results, must be much larger than the disturbance frequency. Thus, the region of validity of Hall's results and the results of Grosch & Salwen (1968) and Herbert (1972) do not necessarily overlap. The degree of destabilization found by Hall is slight. He finds that the critical Reynolds number is reduced by the amount $\delta R \simeq -\Delta^2(21{\cdot}7/\beta)^5 R_c$ for $\beta \to \infty$. Here β is a measure of the oscillation frequency and Δ is the ratio of oscillation velocity to mean velocity amplitude. This result is claimed to be valid for $\beta > 50$. The value $\beta \simeq 40$ corresponds to an imposed oscillation of about twice the frequency of the neutrally stable disturbance mode at the critical point of steady plane Poiseuille flow.

A re-examination of the stability characteristics of OPP flow is made in this study in order to attempt to fill some of the remaining information gaps concerning this stability problem. A particularly interesting and important point that needs to be examined is Grosch & Salwen's (1968) claim that OPP flow is destabilized when the oscillatory velocity amplitude exceeds the value of $0{\cdot}105U_0$, where U_0 is the maximum mean velocity. Grosch & Salwen (1968) conjectured that this destabilization was the result of a resonant coupling between the imposed oscillation (with a frequency equal to the frequency of the principal neutral disturbance) and one of the higher, stable, modes of the mean flow. In this study the stability problem is analysed by a perturbation method which allows the direct evaluation of the effects of the imposed oscillation on each disturbance mode of the underlying steady flow. Thus Grosch & Salwen's result will be examined in order to identify specifically any kind of resonant coupling between the imposed oscillation and particular disturbance modes, or combinations of modes, of the mean flow.

It is also of interest to determine the oscillation frequency which seems to be the most effective in either stabilizing or destabilizing the flow. In particular, the case of low-frequency oscillation may have important applications and thus needs to be examined.

The remainder of this paper is divided as follows: The basic flow and the formulation of the stability problem is described in § 2. The method of solution of the stability problem by a combination of numerical and perturbation techniques is described in § 3. The numerical results for the stability problem are discussed in § 4. Some concluding remarks are made in § 5.

2. Formulation

The two-dimensional flow of a viscous, incompressible, homogeneous fluid between infinite parallel plates is considered. A Cartesian co-ordinate system (x', y', z') is placed with its origin halfway between the plates. The $y' = 0$ plane is parallel to the

plates. The plates intersect the y' axis at the values of $\pm h$. The basic motion of the fluid is forced by the combination of the spatially and temporally constant pressure gradient $-P_0\mathbf{i}$ and the time periodic and spatially constant pressure gradient

$$-Q_0 \cos \omega t' \mathbf{i}.$$

The unit vector $\mathbf{i}$ is tangent to the x axis and ω is the angular frequency of the imposed oscillation.

The flow variables are appropriately scaled by the length h, the velocity $U_0 = h^2 P_0/2\nu$, where ν is the kinematic viscosity of the fluid, the time h/U_0 and the pressure ρU_0^2, where ρ is the density of the fluid. Then the basic fluid velocity $\mathbf{V}$ and pressure P are given by (with $x' = hx$, etc.)

$$\mathbf{V} = (U(y) + \Delta W(y,t), 0, 0), \tag{1a}$$

$$P = -\frac{2x}{R}(1 + \Lambda \cos \Omega t), \tag{1b}$$

where

$$U(y) = 1 - y^2, \tag{2a}$$

$$W(y,t) = \mathscr{R}\left\{\left[\frac{\cosh \beta(1+i) - \cosh \beta(1+i)\, y}{i \cosh \beta(1+i)}\right] e^{i\Omega t}\right\} \tag{2b}$$

and where $i = \sqrt{-1}$, $R = U_0 h/\nu$ is the Reynolds number, $\Lambda = Q_0/P_0$ is the pressure ratio, $\Delta = \Lambda/\beta^2$ is the ratio of the amplitude of the oscillatory to steady velocity, $\beta = h/\delta$ is the ratio of the channel half-width to Stokes-layer thickness $\delta = (2\nu/\omega)^{\frac{1}{2}}$ and $\Omega = h\omega/U_0 = 2\beta^2/R$ is the dimensionless frequency of the imposed oscillatory pressure gradient. It is important to note that at large values of the angular frequency ω the Stokes layers are relatively thin, i.e. β is large and hence the ratio of oscillatory to steady velocity Δ is very small even for fairly large values of the pressure gradient ratio Λ. A high frequency in this context would be the frequency of the principal disturbance modes near the critical point α_c, R_c of the underlying steady flow for which $\beta \simeq 28$.

The basic state (1) is infinitesimally disturbed and the resulting velocity and pressure field must satisfy the constant-density Navier–Stokes equations. Upon linearizing these equations in the usual way of linear stability theory and restricting the disturbances to be two-dimensional and in the plane of the basic motion one obtains for the velocity perturbations $\mathbf{v} = (u, v)$ and pressure perturbation p the equations

$$\partial \mathbf{v}/\partial t + (U + \Delta W)\mathbf{i}.\nabla \mathbf{v} + \mathbf{v}.\nabla(U + \Delta W)\mathbf{i} = -\nabla p + R^{-1}\nabla^2 \mathbf{v}, \tag{3a}$$

$$\nabla . \mathrm{v} = 0, \tag{3b}$$

$$u = v = 0 \quad \text{at} \quad y = \pm 1, \tag{3c}$$

where $\nabla \equiv \mathbf{i}\,\partial/\partial x + \mathbf{j}\,\partial/\partial y$ and $\mathbf{j}$ is a unit vector tangent to the y axis. A Squires theorem guaranteeing that the critical Reynolds number occurs for a two-dimensional disturbance can be proved (see von Kerczek & Davis 1974).

The disturbance equation (3) admits normal mode solutions of the form

$$(u, v, p) = \mathscr{R}(\hat{u}(y,t), \hat{v}, \hat{p})\, e^{i\alpha x}. \tag{4}$$

It is most convenient to work with the stream function $\psi(x, y, t)$, where

$$\psi(x, y, t) = \phi(y, t)\, e^{i\alpha x}, \tag{5}$$

and from which the velocity mode functions $(\hat{u}, \hat{v})$ can be calculated by the formula

$$\hat{u} = \frac{\partial \phi}{\partial y}, \quad \hat{v} = -i\alpha\phi. \tag{6}$$

Accordingly, the two-dimensional disturbance equation (3) becomes the time-dependent Orr–Sommerfeld equation

$$\frac{\partial}{\partial t}\mathscr{L}\phi = \frac{1}{R}\mathscr{L}^2\phi - i\alpha\left(U\mathscr{L}\phi - \frac{d^2U}{dy^2}\phi\right) - i\alpha\Delta\left(W\mathscr{L}\phi - \frac{\partial^2 W}{\partial y^2}\phi\right), \tag{7a}$$

$$\phi = \frac{\partial \phi}{\partial y} = 0 \quad \text{on} \quad y = \pm 1, \tag{7b}$$

where

$$\mathscr{L} \equiv \frac{\partial^2}{\partial y^2} - \alpha^2.$$

When the velocity amplitude ratio Δ is equal to zero, equations (7) describe the stability characteristics of steady plane Poiseuille flow. In this case let $\lambda_{(l,0)}$ be the complex growth rate of the lth disturbance mode.

These modes are ordered in such a way that ascending values of l, starting with $l = 1$, correspond to descending values of $\mathscr{R}(\lambda_{(l,0)})$. The main objective in this work is to compute the change in the complex growth rate $\lambda_{(l,0)}$ as the value of the ratio Δ increases from zero.

By the analogy with Floquet theory for ordinary differential equations (see Coddington & Levinson 1955) solutions of equations (7) will have the form

$$\phi(y, t) = g(y, t)\, e^{\lambda t}, \tag{8}$$

where $g(y, t)$ is a function that is $(2\pi/\Omega)$-periodic in time. The possibility that the mode function $g(y, t)$ in equation (8) is not time-periodic does not have to be considered here because the eigenvalues $\lambda_{(l,0)}$ of the underlying steady basic state are distinct (see Grosch & Salwen 1968). In any case, the stability (instability) of the flow is determined by the condition that $\mathscr{R}(\lambda_{(1)}) < 0$ ($\mathscr{R}(\lambda_{(1)}) \geqslant 0$).

3. The method of solution of the stability problem

The method by which equations (7) are solved, in the form of equation (8) is a combination of a numerical and perturbation procedure in which the Floquet exponent λ and the eigenfunction $g(y, t)$ are computed as series in the velocity amplitude ratio Δ.

Both the steady flow velocity profile U and the time-periodic velocity profile W are symmetric with respect to the $y = 0$ centre-line of the channel. Hence, solutions of equations (7) are either symmetric or antisymmetric with respect to $y = 0$. Such solutions can be treated separately. It has been shown numerically by Grosch & Salwen (1968), Orszag (1971) and others that the only unstable mode of steady plane Poiseuille flow is an even eigenfunction of equations (7) with $\Delta = 0$. Thus, the main concern in this investigation is the effect of the basic flow oscillation on these symmetric eigenfunctions. However, the effects of oscillation on the antisymmetric eigen-

functions have also been explored briefly. It was found that the symmetric flow oscillation induced by the time periodic pressure gradient has almost no effect at all on the antisymmetric eigenfunctions. Hence, no further discussion of this class of solutions of equations (7) is necessary.

The first step used to solve equations (7) is their reduction to a system of ordinary differential equations in time by a Galerkin-like method. The stream function $\phi(y,t)$ is expanded in a Chebyshev polynomial series (see Orszag 1971) with time dependent coefficients as follows:

$$\phi(y,t) = \sum_{n=1}^{N} a_n(t)\, T_{2n-2}(y), \tag{9}$$

where $T_m(y) = \cos(m\cos^{-1}y), m = 0, 1, 2, \ldots$ are Chebyshev polynomials of the first kind. Since only the even Chebyshev polynomials are used in equation (9) the symmetry conditions $\phi_y = \phi_{yyy} = 0$ at $y = 0$ are automatically satisfied. Hence, only the boundary conditions $\phi = \phi_y = 0$ at $y = 1$ need to be imposed on equation (9).

By using the τ-method as described by Orszag (1971) and by using the boundary conditions $\phi = \phi_y = 0$ at $y = 1$ to relate the coefficients a_N and a_{N-1} to the remaining coefficients $a_1, \ldots, a_{N-2}$, the system of ordinary differential equations

$$\mathbf{Q}.\frac{d\mathbf{a}}{dt} = (\mathbf{P} - i\alpha\mathbf{J}).\mathbf{a} - i\alpha\Delta\mathbf{V}.\mathbf{a} \tag{10}$$

is obtained. The system of equations (10) approximates the equations (7) with increasing accuracy as $N \to \infty$. In equation (10) the vector $\mathbf{a} = (a_i)^\dagger$, where the a_i, $i = 1, \ldots, N-2$, are the expansion coefficients of equation (9) and the superscript dagger denotes a column vector in which the free index designates the components of the vector. The $(N-2)\times(N-2)$ term matrices $\mathbf{Q}$, $\mathbf{P}$, $\mathbf{J}$ and $\mathbf{V}$ are the representations of the operators $\mathscr{L}$, $R^{-1}\mathscr{L}^2$, $(U\mathscr{L} - U_{yy})$ and $(W\mathscr{L} - W_{yy})$, respectively, together with the boundary conditions (7*b*) in the Chebyshev basis $T_0, T_2, \ldots, T_{2N-2}$. The matrices $\mathbf{Q}$, $\mathbf{P}$ and $\mathbf{J}$ are constant and $\mathbf{Q}$ is invertible, whereas the matrix $\mathbf{V}$ is $(2\pi/\Omega)$-periodic in time. One can easily obtain numerical solutions of equation (10) by numerical time integration and use of the Floquet theorem although such a procedure incurs a considerable computational expense (see Grosch & Salwen 1968; von Kerczek & Davis 1974). Since the main objective in this work is the determination of the Floquet exponent λ as Δ increases from zero, a perturbation method to construct a series solution in Δ will be used. It will be shown that it is not difficult to compute a considerable number of terms of this series and, with the aid of certain summation techniques, to calculate accurate values of the exponent λ for values of Δ as large as $\frac{1}{4}$.

The general theory of perturbation techniques for calculating the Floquet exponents of systems of equations of type (10) are reviewed in the book of Yakubovich & Starzhinskii (1975). A simpler direct method of expansion for the special case when the matrix $(\mathbf{P} - i\alpha\mathbf{J})$ has a simple spectrum will be described here.

A preliminary step is performed in order to make subsequent calculations simpler. First equation (10) is left-multiplied by the inverse $\mathbf{Q}^{-1}$ of the matrix $\mathbf{Q}$. Let $\mathbf{B}$ be the matrix that diagonalizes the matrix $\mathbf{Q}^{-1}.(\mathbf{P} - i\alpha\mathbf{J})$. Then the new vector of unknown coefficients $\mathbf{b}$ is defined by the equation

$$\mathbf{a} = \mathbf{B}.\mathbf{b}. \tag{11}$$

By substituting equation (11) into equation (10) and by left multiplying the resulting equation by $\mathbf{B}^{-1}$ the equation

$$\frac{d\mathbf{b}}{dt} = \mathbf{D}.\mathbf{b} + \Delta\mathbf{E}.\mathbf{b} \tag{12}$$

is obtained, where

$$\mathbf{D} \equiv \mathbf{B}^{-1}.\mathbf{Q}^{-1}.(\mathbf{P} - i\alpha\mathbf{J}).\mathbf{B} \equiv [\lambda_{(1,0)}, \ldots, \lambda_{(N',0)}], \tag{13a}$$

$$\mathbf{E} \equiv -i\alpha\mathbf{B}^{-1}.\mathbf{Q}^{-1}.\mathbf{V}.\mathbf{B} \equiv \mathbf{E}^{(1)}e^{i\Omega t} + \mathbf{E}^{(-1)}e^{-i\Omega t} \tag{13b}$$

and where $[\lambda_{(j,0)}]$ designates a diagonal matrix. The matrices $\mathbf{E}^{(1)}$ and $\mathbf{E}^{(-1)}$ are complex constant matrices and $N' = N - 2$.

At this point of the exposition it is necessary to describe the system of notation to be used in the rest of this paper. The following analysis will deal with lengthy multiple sequences of vectors and it is important to distinguish between the subscripts and superscripts that denote the position of a vector in a sequence and those that denote a component of a vector. Hence, superscripts and subscripts that designate a term in a sequence will be enclosed in parenthesis but a subscript that designates a component of a vector (or matrix) will stand free outside of the parenthesis. However, a special exception should be noted for the sequence of coefficients $\lambda_{(l,j)}$. This sequence of coefficients and the corresponding sequence of values $\gamma_{(l,j)}$ (to be defined later) will also form the elements of a diagonal matrix and will then occur in formulae in which one of the indices is summed with corresponding components of a vector (see formulae (26) and (28)). However, the context should make clear the role that each of the subscripts play. The index l will be especially reserved to denote the disturbance mode of the steady flow stability problem about which the perturbation due to the imposed oscillation is calculated. Hence l denotes a fixed integer. The summation convention for repeated indices will not be used.

The solutions $\mathbf{b}(t)$ of equation (12) must have the form

$$\mathbf{b}(t) = \mathbf{z}(t)e^{\lambda t}, \tag{14}$$

where $\mathbf{z}(t)$ is $2\pi/\Omega$-periodic in time. The solution (14) is to be computed in terms of the oscillation-induced perturbations to the individual steady flow disturbance modes $\mathbf{z}_{(l,0)}\exp(\lambda_{(l,0)}t)$. Hence, $\mathbf{b}(t)$ is expanded in a series of powers of Δ as follows:

$$\mathbf{z}_{(l)}(t) = \mathbf{z}_{(l0)} + \Delta\mathbf{z}_{(l1)} + \Delta^2\mathbf{z}_{(l2)} + \ldots, \tag{15a}$$

$$\lambda_{(l)} = \lambda_{(l0)} + \Delta\lambda_{(l1)} + \Delta^2\lambda_{(l2)} + \ldots . \tag{15b}$$

By substituting the series (15) into equations (14) and (12) and collecting terms corresponding to each power of Δ yields the following system of perturbation equations:

$$\frac{d\mathbf{z}_{(l0)}}{dt} - (\mathbf{D} - \lambda_{(l0)}\mathbf{I}).\mathbf{z}_{(l0)} = 0, \tag{16}$$

$$\frac{d\mathbf{z}_{(l1)}}{dt} - (\mathbf{D} - \lambda_{(l0)}\mathbf{I}).\mathbf{z}_{(l1)} = \mathbf{E}.\mathbf{z}_{(l0)} - \lambda_{(l1)}\mathbf{z}_{(l0)}, \tag{17a}$$

$$\frac{d\mathbf{z}_{(l2)}}{dt} - (\mathbf{D} - \lambda_{(l0)}\mathbf{I}).\mathbf{z}_{(l2)} = \mathbf{E}.\mathbf{z}_{(l1)} - \lambda_{(l1)}\mathbf{z}_{(l1)} - \lambda_{(l2)}\mathbf{z}_{(l0)}, \tag{17b}$$

$$\frac{d\mathbf{z}_{(lj)}}{dt} - (\mathbf{D} - \lambda_{(l0)}\mathbf{I}).\mathbf{z}_{(lj)} = \mathbf{E}.\mathbf{z}_{(l,j-1)} - \sum_{m=0}^{j-1}\lambda_{(l,j-m)}\mathbf{z}_{(lm)}, \tag{17c}$$

where **I** is the unit matrix. Note that the constant coefficient matrix of these equations is the diagonal matrix

$$\mathbf{D} - \lambda_{(l0)}\mathbf{I} = [\gamma_{(l1)}, \ldots, \gamma_{(l,N')}],$$

where

$$\gamma_{(lj)} \equiv \lambda_{(j0)} - \lambda_{(l0)} \quad \text{for} \quad j = 1, \ldots, N'.$$

The only possible $2\pi/\Omega$-periodic solution of equation (16) is

$$\mathbf{z}_{(l0)} = (\delta_{lj})^{\dagger}, \tag{18}$$

where δ_{lj} is the Kronecker delta and l is a fixed integer. The reason for this is that $\gamma_{(ll)} = 0$ and $\gamma_{(lj)} \neq \pm im\Omega$ when $l \neq j$ and m is an integer.

Since the solution vectors $\mathbf{z}_{(lj)}$, $j = 0, 1, 2, \ldots$, must all be $2\pi/\Omega$-periodic, the inner product $\langle \mathbf{f}, \mathbf{g} \rangle$ defined by

$$\langle \mathbf{f}, \mathbf{g} \rangle \equiv \frac{\Omega}{2\pi} \int_0^{2\pi/\Omega} \sum_{j=1}^{N'} f_j g_j^* \, dt \tag{19}$$

will be needed. The superscript $*$ denotes complex conjugation. Furthermore, the eigenfunction $\mathbf{y}_{(l,0)}$ of the equations adjoint to system (16) will also be needed. This adjoint eigenfunction is

$$\mathbf{y}_{(l,0)} = (\delta_{lj})^{\dagger}. \tag{20}$$

The solution of any one of the equations in the set (17) can be obtained from the solution of its preceding member in the set by the application of the Fredholm alternative and the requirements that these solutions be unique, i.e. they do not contain arbitrary multiples of the eigensolution $\mathbf{z}_{(l,0)}$, and that they are $2\pi/\Omega$-periodic in time.

Let the right-hand side of equation (17*c*) be designated as $\mathbf{h}_{(j)}(t)$ and note that $\mathbf{h}_{(j)}(t)$ can be represented by a Fourier series. Thus, let

$$\mathbf{h}_{(j)}(t) = \sum_{k=-\infty}^{\infty} \mathbf{h}_{(jk)} e^{ik\Omega t}, \tag{21}$$

where the vectors $\mathbf{h}_{(jk)}$ are constant vectors and the lth component, $h_{(j0)l}$, of the vector $\mathbf{h}_{(j0)}$ is zero. This property is enforced by the solution procedure for equations (17).

In order that equation (17*c*) has a solution, the vector $\mathbf{h}_{(j)}(t)$ must satisfy the orthogonality condition

$$\langle \mathbf{h}_{(j)}(t), \mathbf{y}_{(l0)} \rangle = 0. \tag{22}$$

The satisfaction of this condition is achieved by properly selecting the value of the parameter $\lambda_{(lj)}$. Then the general solution of equation (17*c*) can be written as

$$\mathbf{z}_{(lj)} = e^{[\gamma_{(l,i)}]t} \left\{ \boldsymbol{\xi}_0 + \int_0^t e^{-[\gamma_{(l,i)}]s} . \mathbf{h}_{(j)}(s) \, ds \right\}. \tag{23}$$

Formula (23) is easily evaluated because the matrix $[\gamma_{(l,i)}]$ is diagonal. By requiring that $\mathbf{z}_{(lj)}(t)$ be unique and $(2\pi/\Omega)$-periodic in time values of $\boldsymbol{\xi}_0$ are obtained which eliminate all the non-$(2\pi/\Omega)$-periodic functions and the multiples of the vector $\mathbf{z}_{(l0)}$ from the solution $\mathbf{z}_{(lj)}$. The result of this calculation is

$$\mathbf{z}_{(lj)}(t) = \sum_{k=-\infty}^{\infty} \left(\frac{h_{(kj)m}}{ik\Omega - \gamma_{(lm)}} \right)^{\dagger} e^{ik\Omega t}. \tag{24}$$

The solutions of the entire set of equations (17) can now be obtained in sequence, starting with equation (17a), by first computing the right-hand side $\mathbf{h}_{(j)}$, then calculating the required value of $\lambda_{(lj)}$ using equation (22) and then calculating the solution $\mathbf{z}_{(lj)}$ by equation (24). The most laborious aspect of this computation is the calculation of the vector $\mathbf{h}_{(jk)}$. A procedure has been coded (in Fortran IV) to compute $M = 40$ terms of the series (15). More terms can be computed by simply changing certain dimension statements in this code, but 40 terms (with $N = 35$) seemed to be the largest number that the storage capacity of the DEC-10 computer system could accommodate conveniently. The first two perturbation terms of the series (15) are given below to illustrate the form of these solutions:

$$\lambda_{(l1)} = 0, \tag{25a}$$

$$\mathbf{z}_{(l1)} = \boldsymbol{\zeta}^{(1)}_{(l1)} e^{i\Omega t} + \boldsymbol{\zeta}^{(-1)}_{(l1)} e^{-i\Omega t}, \tag{25b}$$

where

$$\boldsymbol{\zeta}^{(1)}_{(l1)} \equiv \left(\frac{E^{(1)}_{jl}}{i\Omega - \gamma_{(lj)}} \right)^{\dagger}, \tag{26a}$$

$$\boldsymbol{\zeta}^{(-1)}_{(l1)} \equiv \left(\frac{-E^{(-1)}_{jl}}{i\Omega + \gamma_{(lj)}} \right)^{\dagger} \tag{26b}$$

$$\lambda_{(l2)} = \sum_{j=1}^{N'} (E^{(1)}_{lj} \zeta^{(-1)}_{(l1)j} + E^{(-1)}_{lj} \zeta^{(1)}_{(l1)j}), \tag{27a}$$

$$\mathbf{z}_{(l2)}(t) = \sum_{k=-2}^{2} \boldsymbol{\zeta}^{(k)}_{(l2)} e^{ik\Omega t}, \tag{27b}$$

where

$$\boldsymbol{\zeta}^{(2)}_{(l2)} \equiv \left(\frac{\sum_{j=1}^{N'} E^{(1)}_{mj} \zeta^{(1)}_{(l1)j}}{2i\Omega - \gamma_{(lm)}} \right)^{\dagger}, \tag{28a}$$

$$\boldsymbol{\zeta}^{(0)}_{(l2)} \equiv \left(\frac{\left(\sum_{j=1}^{N'} (E^{(1)}_{mj} \zeta^{(-1)}_{(l1)j} + E^{(-1)}_{mj} \zeta^{(1)}_{(l1)j}) - \lambda_{(l2)} \delta_{lm} \right)}{-\gamma_{(lm)}} \right)^{\dagger}, \tag{28b}$$

$$\boldsymbol{\zeta}^{(-2)}_{(l2)} \equiv \left(\frac{\sum_{j=1}^{N'} E^{(-1)}_{mj} \zeta^{(-1)}_{(l1)j}}{-2i\Omega - \gamma_{(lm)}} \right)^{\dagger}, \tag{28c}$$

$$\boldsymbol{\zeta}^{(\pm 1)}_{(l2)} \equiv 0, \tag{28d}$$

and where

$$(E^{(\pm 1)}_{lj}) \equiv \mathbf{E}^{(\pm 1)}.$$

Note that the order-Δ perturbation $\lambda_{(l1)}$ of the eigenvalue $\lambda_{(l0)}$ is zero so that the long-term effect of the flow oscillation with amplitude Δ is only of order Δ^2. In fact, all the odd-order perturbation coefficients $\lambda_{(lj)}$, $j = 1, 3, 5, \ldots$, are zero because each eigenvalue $\lambda_{(l0)}$ of the steady Orr–Sommerfeld equation for plane Poiseuille flow is of multiplicity 1 and $\lambda^{*}_{(l0)}$ is not a simultaneous eigenvalue. If $\lambda^{*}_{(l0)}$ were also an eigenvalue of this same equation, as occurs for plane Couette flow above a certain value of the Reynolds number, then the odd-order coefficients $\lambda_{(l,j)}, j = 1, 3, 5, \ldots$, would not be

zero. The examination of the eigensolutions (26), (27) and higher-order terms reveals that the quantities $ni\Omega \pm \gamma_{(lm)}$ for $n = 1, \ldots, N$ appear in the denominators of these solutions. If $ni\Omega \pm \gamma_{(lm)} = 0$ for some values of n and m then resonance at the nth harmonic of the difference frequency $\mathscr{I}(\lambda_{(m0)} - \lambda_{(l0)})$ occurs. In the case considered here $ni\Omega \pm \gamma_{(lm)} \neq 0$ for any value of m or n because $\mathscr{R}\gamma_{(lm)} \neq 0$ for all values of m except for $m = l$, but then $\gamma_{(ll)} = 0$. However, it might be expected that values of Ω near possible resonance, i.e. $\mathscr{I}(ni\Omega \pm \gamma_{(lm)}) = 0$, may cause the values of $\lambda_{(ln)}$ to be large. It will be shown later that this does not seem to occur.

It cannot be expected that the series (15) is convergent for all values of Δ. Estimates of the radius of convergence of series (15*b*) can be obtained by computing the Neville table (see Gaunt & Guttmann 1974) from the coefficients $\lambda_{(lj)}, j = 0, \ldots, M$. The Neville table (which is a generalization of the Domb–Sykes plot) also yields estimates of the actual value of the nearest singularity and its exponent, but this information will not be used here (see Van Dyke 1974, for techniques of analysis of series coefficients in fluid mechanics).

The value of the function $\lambda_{(ll)}(\Delta)$ can be obtained for the values of Δ well beyond the radius of convergence of the series (15*b*) by recasting it into different kinds of approximations. For example, the series (15*b*) can be recast into various Padé fractions which yield the same order of approximation of $\lambda_{(ll)}(\Delta)$ as the series (15*b*) near the origin $\Delta = 0$ and possibly better approximations of $\lambda_{(ll)}(\Delta)$ for larger values of Δ. Alternatively, the nonlinear sequence transformations for summing series, such as Shanks' transformation (Shanks 1955), can yield accurate values of $\lambda_{(ll)}(\Delta)$ from the series (15*b*) well beyond its radius of convergence.

Recently, Vanden-Broeck & Schwartz (1979) have given a very simple one-parameter family of sequence transformations for summing a M-term series that has the Shanks transformation and the values of the entire K/L ($K + L + 1 = M$) Padé table imbedded in it. In the present work the sequence of partial sums of series (15*b*) for specific values of Δ were transformed using several members of the Vanden-Broeck–Schwartz family of transformations. It was found that the Shanks transformation, given by

$$S_{(n,m+1)} \equiv \frac{S^2_{(n,m)} - S_{(n-1,m)} S_{(n+1,m)}}{2S_{(n,m)} - S_{(n-1,m)} - S_{(n+1,m)}} \tag{29}$$

where

$$S_{(n,0)} \equiv \sum_{j=0}^{n} \lambda_{(l,2j)} \Delta^{2j}, \tag{30}$$

invariably gives the best results. The triangular table of values $S_{(n,m)}$ is expected to convergence along the diagonals. The element $S_{(P,P)}$, where $P = [\frac{1}{2}M] + 1$, at the apex of the triangular array $S_{(n,m)}$ of numbers is assumed to be the value of the function $\lambda_{(ll)}(\Delta)$.

4. Computational results

There are four independent dimensionless parameters, α, R, β and Δ, in this stability problem. Thus, it is difficult to map completely the stability characteristics of OPP flow in this parameter space. Instead, only a sample set of results were computed in the parameter range which seems to provide a fairly good picture of the effects of

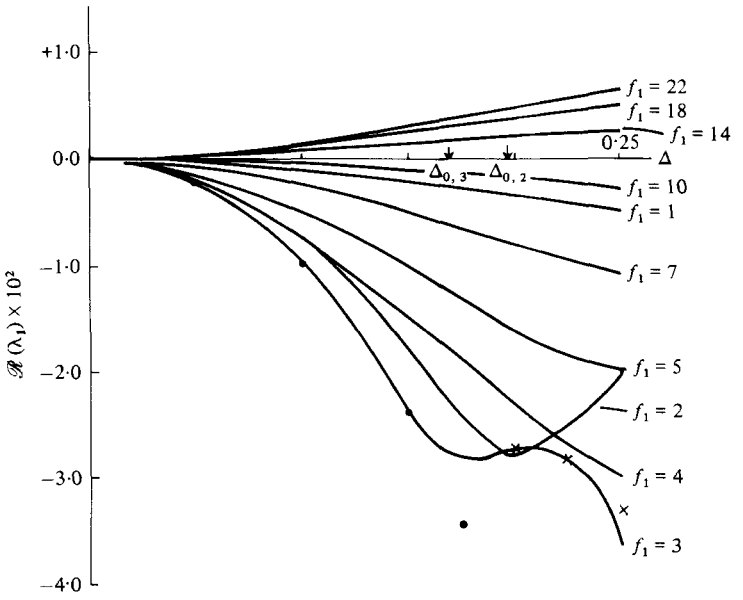

FIGURE 1. The value of the principal disturbance growth rate $\mathscr{R}(\lambda_1)$ as a function of Δ for various values of $f_1 = \omega_1/\Omega$ at $R = 5772{\cdot}22$, $\alpha = 1{\cdot}0206$. The values of $\mathscr{R}(\lambda_1)$ for $f_1 = 3$ that were obtained by numerical time integration are denoted by $\times$. The values of $\mathscr{R}(\lambda_1)$ for $f_1 = 3$ that were obtained by the simple sum of the series (14*b*) are denoted by ●.

oscillating the plane Poiseuille flow. The values of the parameters that were chosen correspond to ways in which the oscillation of plane Poiseuille flow might be imposed experimentally. For example, the effects of the oscillations on the stability characteristics were examined for fixed values of the dimensional oscillation frequency (i.e. β is fixed) rather than for fixed values of the dimensionless frequency Ω. Similarly, when examining the effects of oscillation amplitude at fixed values of β but various values of R, it seems that it is best to keep the dimensional pressure gradient Q_0 fixed at the value of Q_f. Hence, the dimensionless pressure gradient amplitude Λ varies as $\Lambda = \Lambda_f R_f/R$ where Λ_f is the reference value of Λ corresponding to Q_f at the value of Reynolds number R_f. In this case, the oscillation amplitude Δ varies like $\Delta = \Delta_f R_f/R$ where $\Delta_f = 2\Lambda_f/\beta^2$. For these reasons some of the results presented below are not directly comparable with the results of Grosch & Salwen (1968).

The first set of results to be described concern the effects of the imposed oscillation on the disturbance modes of the steady flow at the critical point $\alpha = \alpha_c \equiv 1{\cdot}0206$, $R = R_c \equiv 5772{\cdot}22$. Figure 1 shows graphs of the growth rate, $\mathscr{R}(\lambda_{(1)})$, of the principal disturbance mode as a function of the oscillation velocity amplitude ratio Δ. Graphs for various values of the disturbance to imposed frequency ratio ω_1/Ω, where $\omega_1 \equiv \mathscr{I}(\lambda_{(1,0)})$, are shown in the figure. These numerical results were obtained with $M = 20$ to 40 terms of the series (15). The two arrows in figure 1, which are designated Δ_{02} and Δ_{03}, indicate the radius of convergence of the series (15*b*) for the cases $\omega_1/\Omega = 2$ and 3 respectively. The values of Δ_{02} and Δ_{03} as well as similar values for all the other cases in figure 1, were computed by calculating the first three columns of the Neville table. The first column of the Neville table corresponds to linear extrapolation to a value of $1/M = 0$ of the points of the Domb–Sykes plot (see Van Dyke 1974). Subse-

I	$\mathscr{R}(\lambda'_{(1,j)})$	$\mathscr{I}(\lambda'_{(1,j)})$ $(j = 2I-2)$
1	−0·0000004D−02	−0·2694449D+00
2	−0·2190788D+00	0·2937376D−01
3	−0·4946925D+00	0·3337881D+00
4	−0·1665550D+01	0·2707253D+01
5	−0·3312176D+01	0·2016428D+02
6	0·2912503D+02	0·1392865D+03
7	0·5551554D+03	0·8725125D+03
8	0·6165819D+04	0·4653925D+04
9	0·5641097D+05	0·1682281D+05
10	0·4544982D+06	−0·3039907D+05
11	0·3253154D+07	−0·1466197D+07
12	0·2006811D+08	−0·1985873D+08
13	−0·9468543D+08	−0·2043690D+09
14	0·1392515D+09	−0·1804071D+10
15	−0·4038728D+10	−0·1405346D+11
16	−0·7061911D+11	−0·9549242D+11
17	−0·8120626D+12	−0·5286387D+12
18	−0·7744830D+13	−0·1732335D+13
19	−0·6461354D+14	0·8907986D+13
20	−0·4733939D+15	0·2550031D+15
21	−0·2929473D+16	0·3343126D+16

TABLE 1. The coefficients of series (15*b*) for $\alpha = 1{\cdot}0206$, $R = 5772{\cdot}22$, $\omega_1/\Omega = 3{\cdot}0$ ($\beta = 16{\cdot}1$), $N = 28$, $\lambda_{(1,j)} = 2^j\lambda'_{(1,j)}$

quent columns of the Neville table represent higher-order extrapolations of these points. The last value of each of the first three columns of the Neville table, in each of the cases graphed in the figure, agreed to at least three significant figures. It was found that this procedure of estimating the radius of convergence of the series (15*b*) is very accurate. In all the cases that were examined, Cauchy convergence of the partial sums of series (15*b*) could be achieved to at least four or five significant figures for values of Δ up to about 95 % of the values Δ_0, where Δ_0 designates the predicted value (by the Neville table) of the radius of convergence of series (15*b*). In the worst case, that of $\omega_1/\Omega = 3$, convergent values (at least in the Cauchy sense) of $\mathscr{R}(\lambda_{(1)})$ could be obtained for values of Δ up to 135 % of the value of Δ_{03} by applying the Shanks transformation to series (15*b*). Table 1 gives the coefficients $\lambda_{(1,j)}$ for the case $\omega_1/\Omega = 3$, $\alpha = \alpha_c$, $R = R_c$, $N = 28$ and $M = 40$. These coefficients were obtained in multiple precision (25 decimal digit mantissa) and rounded to 7 significant figures. Figure 1 shows values of $\mathscr{R}(\lambda_{(1)})$, for the case $\omega_1/\Omega = 3$, that were obtained by a numerical time integration of the differential equations (12). These values are designated by crosses. Note the excellent agreement of these values of $\mathscr{R}(\lambda_{(1)})$ with the values predicted by the convergent terms of the Shanks-transformed sums of series (15*b*) up to values of $\Delta = 0{\cdot}225$.

The significance of the results shown in figure 1 is that in the frequency range $\Omega > \frac{1}{10}\omega_1$ (recall that $\omega_1 = 0{\cdot}2694$) the imposed oscillation has only a stabilizing effect on the principal disturbance mode of the underlying steady flow. The fairly low-

l	$\lambda_{(l,0)}$	$\mathscr{R}(\lambda_{(l,2)})$	$\mathscr{R}(\lambda_{(l,4)})$
1	$0{\cdot}0 + i\,0{\cdot}2694$	$-0{\cdot}1072$	$0{\cdot}3056$
2	$-0{\cdot}0467 + i\,0{\cdot}9736$	$O(10^{-9})$	$O(10^{-9})$
3	$-0{\cdot}0839 + i\,0{\cdot}9360$	$O(10^{-8})$	$O(10^{-8})$
4	$-0{\cdot}1211 + i\,0{\cdot}8983$	$O(10^{-7})$	$O(10^{-6})$
5	$-0{\cdot}1555 + i\,0{\cdot}4119$	$-0{\cdot}3124$	$1{\cdot}699$
6	$-0{\cdot}1583 + i\,0{\cdot}8607$	$O(10^{-6})$	$O(10^{-5})$
7	$-0{\cdot}1955 + i\,0{\cdot}8230$	$O(10^{-4})$	$O(10^{-3})$
8	$-0{\cdot}2126 + i\,0{\cdot}2324$	$0{\cdot}5152$	$-0{\cdot}7184$
9	$-0{\cdot}2327 + i\,0{\cdot}7854$	$-0{\cdot}0012$	$0{\cdot}016$
10	$-0{\cdot}2492 + i\,0{\cdot}5637$	$0{\cdot}140$	$0{\cdot}0528$
11	$-0{\cdot}2689 + i\,0{\cdot}7484$	$-0{\cdot}0072$	$-0{\cdot}0144$
12	$-0{\cdot}2762 + i\,0{\cdot}4520$	$0{\cdot}0852$	$-1{\cdot}696$

TABLE 2. The first twelve, mean-flow disturbance exponents and the corresponding first two, non-zero perturbations of the exponent $\mathscr{R}(\lambda_{(l)})$ for $\Omega = \omega_1$, $\alpha = \alpha_c$, $R = R_c$ and $\beta = 27{\cdot}89$

frequency cases $\Omega < \omega_1/10$ result in a slight destabilization of the principal disturbance mode. These results will be discussed later in this section.

Grosch & Salwen (1968) assert that this flow at $\alpha = \alpha_c$, $R = R_c$ becomes unstable for $\omega_1/\Omega = 1$ and $\Delta = 0{\cdot}105$ because one of the higher stable modes of the underlying steady flow is strongly affected by the imposed oscillations. In order to test this claim calculations were made to determine $\lambda_{(l)}$ for $l = 1, 2, \ldots, 12$. Table 2 lists the first twelve eigenvalues $\lambda_{(l,0)}$ (obtained with $N = 34$ terms in the Chebyshev expansion, (9)). One should note that all except the fifth, eighth and twelfth are high-frequency modes compared to the first mode. Furthermore, all the disturbances except the first are fairly heavily damped and thus would require fairly large values of $\mathscr{R}(\lambda_{(l,2)})$ to be significantly altered for such a small value of Δ as $0{\cdot}105$. Table 1 also lists the first two perturbation coefficients to the damping rates, $\mathscr{R}(\lambda_{(l,2)})$ and $\mathscr{R}(\lambda_{(l,4)})$, for each of the first twelve modes and for the value of $\Omega = \omega_1$. The high-frequency disturbance modes are essentially unaffected by the imposed oscillations and although mode 8 has its damping rate reduced none of these disturbances are destabilized. The decay-rate perturbation $\mathscr{R}(\lambda_{(8,2)})\,\Delta^2$ is too small to overcome the very strong damping

$$\mathscr{R}(\lambda_{(8,0)}) = -0{\cdot}2126$$

of mode 8.

For each of the modes listed in table 2 at least $M = 14$ (i.e. the first seven even coefficients $\lambda_{(l,j)}$ terms of series (15*b*) were computed. The number of terms $\lambda_{(l,j)}$ that were computed for each case was sufficient to yield converged values (with the help of the Shanks transformation) of $\lambda_{(l)}$ from series (15*b*) for values of Δ at least as large as $0{\cdot}3$. The first two terms, $\mathscr{R}(\lambda_{(l,2)})$ and $\mathscr{R}(\lambda_{(l,4)})$ shown in table 2 are adequate for computing accurate values of $\mathscr{R}(\lambda_{(l)})$ for values of Δ up to at least $0{\cdot}15$.

None of the modes in table 2, except the first, is significantly altered for values of Δ up to at least $0{\cdot}3$. On the basis of these results (and also many other similar results that were obtained at other values of α, R and β) it is safe to conjecture that none of the infinite set of higher modes is significantly affected by the imposed oscillations. Thus, these calculations indicate that sinusoidal oscillation with amplitude $\Delta \leqslant 0{\cdot}3$ of plane Poiseuille flow at $R = R_c$ and with frequency $\Omega = \omega_1$ has an overall stabilizing effect on the significant disturbance modes with wavenumber $\alpha = \alpha_c$. Higher modes

ω_1/Ω	β	$\mathscr{R}(\lambda_{(1,2)})$	$\mathscr{R}(\lambda_{(1,4)})$
$\frac{1}{2}$	39·44	−0·011 04	0·019 8
$\frac{1}{4}$	55·77	−0·001 32	0·000 64
$\frac{1}{8}$	78·87	$-4{\cdot}22\times10^{-5}$	$0{\cdot}74\times10^{-5}$
$\frac{1}{16}$	111·5	$1{\cdot}15\times10^{-5}$	$-3{\cdot}5\times10^{-7}$

TABLE 3. High-frequency perturbation coefficients for $\alpha = \alpha_c$ and $R = R_c$

are not strongly affected by the imposed oscillations because of at least one but usually two of the following reasons. The first reason is that the disturbance frequency is so high that there is too large a mismatch between it and the oscillation frequency. Secondly, if the oscillation frequency is as high as the disturbance frequency, then the imposed oscillation vorticity is too closely confined to the boundaries to have an effect on the disturbance. A third reason is that the disturbance is so heavily damped without the oscillation that the small oscillation-induced perturbation cannot overcome this natural damping.

The effects of very-high-frequency imposed oscillations on the principal disturbance mode at $\alpha = \alpha_c$ and $R = R_c$ are shown in table 3. These results show that by increasing the frequency of the imposed oscillations to very large values the oscillatory flow becomes less stable than the steady plane Poiseuille flow. This result is in accord with Hall's (1974) result that for very large values of β the critical Reynolds number R_{sc} of the oscillatory flow is lower than R_c by the amount

$$R_{sc} - R_c = -(21{\cdot}7/\beta)^5 R_c \Delta^2. \tag{31}$$

It can be shown (see equation (38) below) that for small values of Δ and any values of β the difference between R_{sc} and R_c can be obtained from the formula

$$R_{sc} - R_c = \left[\mathscr{R}(\lambda_{(1,2)})_c / \mathscr{R}\left(\frac{d\lambda_{(1,0)}}{dR}\right)_c\right]\Delta^2. \tag{32}$$

By evaluating both of these formulas with the value of $\beta = 111{\cdot}5$ (see tables 3 and 4) one obtains for $(R_{sc} - R_c)/\Delta^2$ the value of about 1·6 from equation (31) and the value of about 7 from equation (32). These values are not inconsistent and may indicate that Hall's formula (31) is only valid for values of β that are very large.

At this point the question of the resolution of the very thin Stokes layers that are present for large values of β must be discussed. Gottlieb & Orszag (1978) show that boundary layers of thickness δ at the ends of the interval $-1 \leqslant y \leqslant 1$ are resolved to within a 1 % maximum pointwise error by Chebyshev expansions with $N = O(3/\sqrt{\delta})$ terms. Thus for the value of $\beta = 111{\cdot}5$ it would seem that $N = 32$ would adequately resolve the thin Stokes layers ($\delta = O(1/\beta)$) at the walls of the channel. Some tests of the variation of the values of $\mathscr{R}(\lambda_{(1,2)})$ with truncation number N were performed.

For the cases $\omega_1/\Omega = \frac{1}{2}$ and $\frac{1}{4}$ there was no variation of the values of $\mathscr{R}(\lambda_{(1,2)})$ or $\mathscr{R}(\lambda_{(1,4)})$ from the values shown in table 3 for $N = 28$, 32 and 34. The values of $\mathscr{R}(\lambda_{(1,2)})$ and $\mathscr{R}(\lambda_{(1,4)})$ for $\omega_1/\Omega = \frac{1}{8}$ and $\frac{1}{16}$ shown in table 3 were obtained using $N = 35$ terms in the Chebyshev expansions. For $N = 32$ Chebyshev terms the values of

$$\mathscr{R}(\lambda_{(1,2)}) = -0{\cdot}417\times10^{-4} \quad \text{and} \quad 1{\cdot}19\times10^{-5}$$

and

$$\mathscr{R}(\lambda_{(1,4)}) = 7{\cdot}31\times10^{-6} \quad \text{and} \quad -3{\cdot}6\times10^{-7}$$

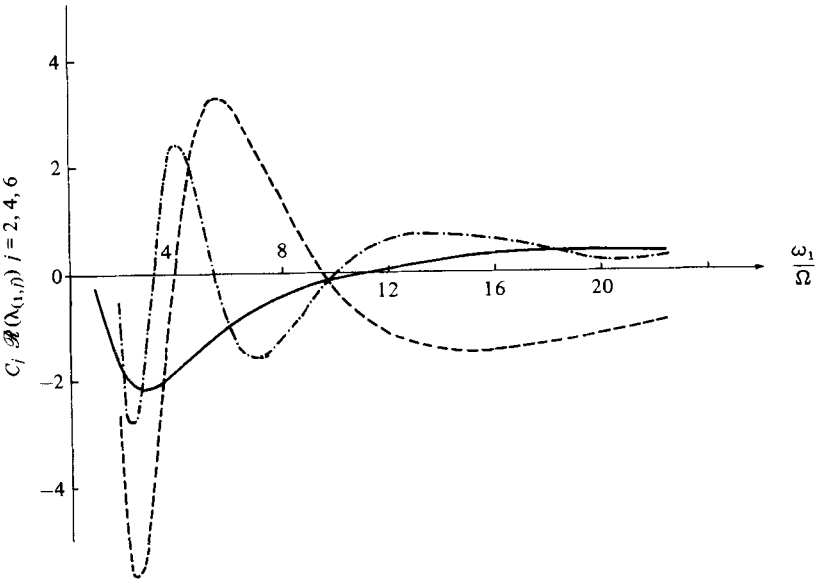

FIGURE 2. The values of $\mathscr{R}(\lambda_{(1,2)})$, $\mathscr{R}(\lambda_{(1,4)})$ and $\mathscr{R}(\lambda_{(1,6)})$ as a function of ω_1/Ω for $R = 5772{\cdot}22$ and $\alpha = 1{\cdot}0206$. $j = 2$, ——, $C_2 = 2{\cdot}5$; $j = 4$, – – –, $C_4 = 0{\cdot}625$; $j = 6$, – · –, $C_6 = \frac{1}{64}$.

were obtained for $\omega_1/\Omega = \frac{1}{8}$ and $\frac{1}{16}$ respectively. These numerical results do seem to indicate that convergence to at least one significant figure has been attained.

Figure 2 shows the graphs of $\mathscr{R}(\lambda_{(1,i)})$ for $i = 2, 4, 6$ in the expansion (15*b*) of $\lambda_{(1)}$ at $\alpha = \alpha_c$ and $R = R_c$ versus the frequency ratio ω_1/Ω. These results were computed in order to study the behaviour of the principal disturbance mode as a function of frequency of the imposed oscillations. Figure 2 shows that there seems to be no identifiable resonance between disturbances and the imposed oscillation. Higher-order perturbation coefficients, $\lambda_{(1,i)}$, $i > 6$, were also computed but are not shown because they do not reveal any particular resonance responses either. Thus, the apparent optimally stabilizing frequency of $\omega_1/\Omega \approx 3$ indicated in figure 1 is not due to any identifiable resonance mechanism.

It has been mentioned in the introduction that it is of interest to examine the effects of fairly-low-frequency imposed oscillations. Thus, some special calculations were made for values of $\omega_1/\Omega = 14$, 18 and 22. Figure 1 shows the changes in the values of $\mathscr{R}(\lambda_{(1)})$ at $\alpha = \alpha_c$ and $R = R_c$. The first eigenmode $\lambda_{(1)}$ is the only one significantly affected by the imposed oscillations even at these very low values of frequency Ω. In these cases, the flow is slightly destabilized. It is important to note that the Floquet exponents $\lambda_{(j)}$ are measures of the *average long-term growth* (or decay) of disturbances. But the Floquet exponent gives no indication of the transient behaviour of a disturbance during one cycle of the imposed oscillation. It has been observed by Rosenblat & Herbert (1970), Finucane & Kelly (1976) and Davis (1976) that at very-low-frequency modulation of a flow it may be much more important to examine the instantaneous relative magnitude and growth rate of a disturbance rather than the Floquet exponent. The reason is that it is possible for disturbances to reach very large instantaneous amplitudes in the early stages of their existence even though over many cycles of modulation they decay in amplitude (see, for example, Finucane & Kelly 1976). Thus,

for the case of $\omega_1/\Omega = 14$ and $\Delta = 0{\cdot}25$ in figure 1, the disturbance equations (12) were integrated numerically over one period $2\pi/\Omega$ of the imposed oscillation.

The disturbance eigenfunction $\mathbf{z}_{(l)}(t)$ can be computed directly by the series (15) since all the vectors $\mathbf{z}_{(l,i)}(t)$, $i = 0, \ldots, M$, are always calculated along with the coefficients $\lambda_{(l,i)}$. However, the evaluation of the series (15*a*) is a non-trivial task in view of the necessity of summing each component using the Shanks transformation. Hence, it was deemed much simpler and computationally not too expensive to simply integrate equation (12), starting with arbitrary initial conditions, over several periods $2\pi/\Omega$. Eventually, the principal mode $\mathbf{z}_{(1)}(t)$ will emerge from this numerical integration. In fact, the principal mode emerges after only one period of integration. Hence, the time history of the solution $\mathbf{z}(t)$ obtained in the second period of integrating equations (12) is an excellent approximation of the principal mode $\mathbf{z}_{(1)}(t)$. A numerical check of this result is available. Let ϵ designate the Euclidean norm

$$\epsilon(t) \equiv \left(\sum_{n=1}^{N} |z_n(t)|^2\right)^{\frac{1}{2}} \Big/ \left(\sum_{n=1}^{N} |z_n(0)|^2\right)^{\frac{1}{2}} \tag{33}$$

of the vector $\mathbf{z}_{(1)}(t)$, where z_n, $n = 1, \ldots, N$, are the components of the vector $\mathbf{z}_{(1)}(t)$. Then

$$\mathscr{R}(\lambda_{(1)}) = \frac{\Omega}{2\pi} \ln\left(\epsilon\left(\frac{2K\pi}{\Omega}\right) \Big/ \epsilon\left(\frac{2(K-1)\pi}{\Omega}\right)\right) \tag{34}$$

for $K \to \infty$. Condition (34) was found to be satisfied to three significant figures at the end of the second period $K = 2$ compared with the value of $\lambda_{(1)}$ computed by series (15*b*) and the Shanks transformation. Furthermore, the numerical integration of equations (12) was continued over the third complete period $2\pi/\Omega$. The computed values of $\epsilon(t)$ and $G(t)$ (defined below) differed by less than one figure in six from the values of ϵ and G at corresponding instants of time in the second period.

Figure 3 shows the time history of the logarithm (base 10) of $\epsilon(t)$ of the mode $\mathbf{z}_{(1)}(t)$ over one period $2\pi/\Omega$ of the imposed oscillation. It can be seen that the disturbance $\mathbf{z}_1(t)$ first decays to a rather small value over the first half of the period and then grows again over the second half of the period. It is noteworthy that this disturbance changes its magnitude by a factor of 10^4 over the second half of the period. This indicates that if the flow is disturbed in the early part of the second half of the imposed oscillation cycle by a moderate amplitude disturbance (but one that may still be considered within the realm of linear theory) then such a disturbance would grow to be so large before the end of the period as to probably lead to transition to turbulence or at least to nonlinear oscillations of the flow.

It is of interest to determine if the decay and growth of this disturbance is mainly a response to the quasi-steady stability characteristics of this flow or whether the disturbance's response is influenced by other factors. Hence, the instantaneous growth rate $G(t)$ defined by

$$G(t) \equiv \frac{1}{\epsilon}\frac{d\epsilon}{dt} \tag{35}$$

was also computed. Figure 4 shows the graph of $G(t)$ versus t over one period $2\pi/\Omega$.

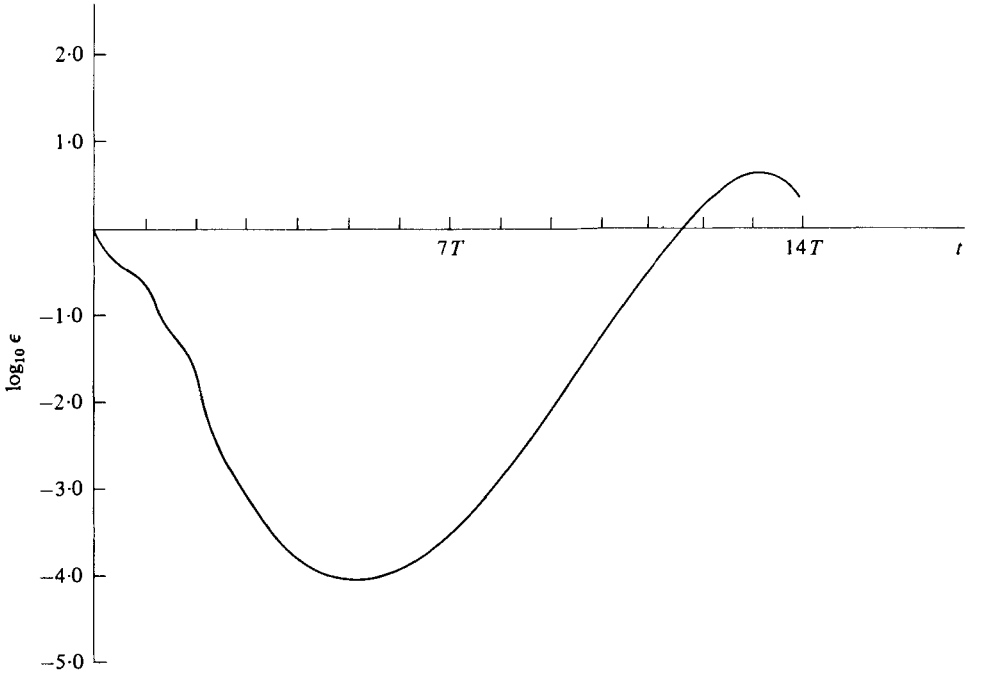

FIGURE 3. The time history of the logarithm of the disturbance norm $\epsilon(t)$ (see (34)) over one period of the basic flow oscillation for $\omega_1/\Omega = 14$ at $R = 5772{\cdot}22$, $\alpha = 1{\cdot}0206$, $\Delta = 0{\cdot}25$ ($T = 2\pi/\omega_1$).

The points designated by the dots are the values of the principal quasi-steady growth (or decay) rate σ of the oscillating flow, where

$$\sigma(t) := \max_{1\leqslant j\leqslant N'} \{\mathscr{R}\sigma_j \,|\, \sigma_j = \text{any eigenvalue of } \mathbf{Q}^{-1}.[\mathbf{P} - i\alpha\mathbf{J} - i\alpha\Delta\mathbf{V}(t)]\}. \tag{36}$$

Although the average behaviour of the instantaneous growth rate $G(t)$ roughly follows the behaviour of the quasi-steady growth rates, there is a significant difference between these quantities. In particular, the erratic behaviour of G in the first quarter of the oscillation indicates that the disturbance undergoes some kind of internal readjustment in the beginning of each cycle of the imposed oscillation. This internal readjustment can be attributed to mode crossings of the quasi-steady eigenvalues σ_j in equation (36). At the value of $t = 0$, $\sigma = \mathscr{R}\sigma_1 = \mathscr{R}(-0{\cdot}04 + i0{\cdot}48)$, but at $t = 0{\cdot}18T$ (where $T = 2\pi/\omega_1$) the second quasi-steady mode, $\sigma_2 = -0{\cdot}047 + i1{\cdot}0$, suddenly becomes the least stable and remains so until $t = 3{\cdot}75T$. During this time interval the first quasi-steady mode has the value $\sigma_1 \simeq -0{\cdot}05 + i0{\cdot}4$. For values of $t > 3{\cdot}75T$ the first mode σ_1 becomes dominant again and by the time $t > 6T$ it becomes unstable. The value of the second mode's decay rate remains about $-0{\cdot}05$ throughout the oscillation cycle. The high-frequency oscillations between $t = 0$ and $4T$ of the solution of the unsteady stability problem is probably due to the second quasi-steady mode (possibly interacting with the first mode) whose frequency is roughly three times the frequency of the first mode. It seems clear that the behaviour of the disturbance is dominated by a combination of the quasi-steady growth rates. However, the main point is that the transient behaviour of a disturbance can be very dangerous (in the

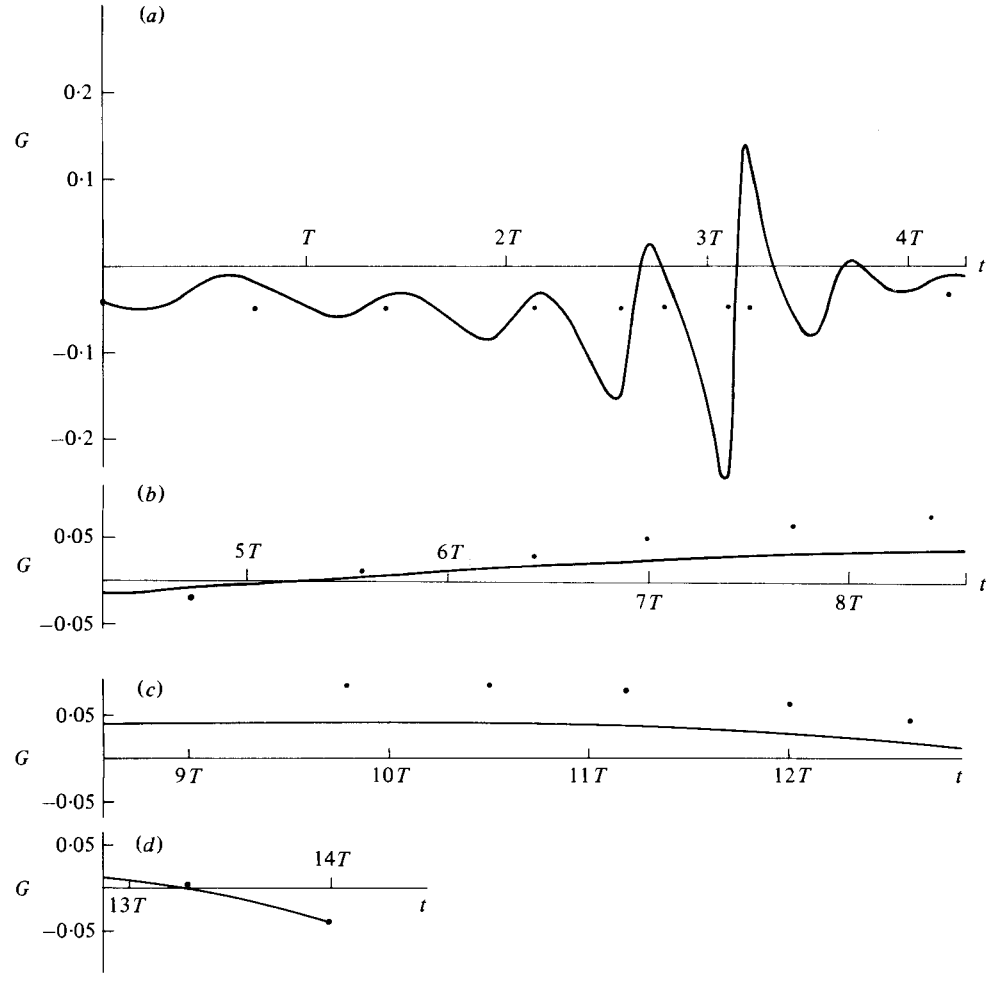

FIGURE 4. The time history of the instantaneous growth rate $G(t)$ (see (35)) for $\omega_1/\Omega = 14$ at $R = 5772{\cdot}22$, $\alpha = 1{\cdot}0206$, $\Delta = 0{\cdot}25$ ($T = 2\pi/\omega_1$). Note that (*b*) is a continuation of (*a*), (*c*) a continuation of (*b*) and (*d*) a continuation of (*c*).

sense that the flow may readily undergo transition to turbulence) even though the long-term average growth rate of the disturbance is very small.

The only experimental results describing the behaviour of small disturbances in an oscillatory shear flow that are available are the measurements by Miller & Fejer (1964) and Obremski & Fejer (1967). These studies were concerned mainly with measurement of laminar to turbulent transition of the oscillatory flat-plate boundary layer. Hence, their results are not directly related to anything studied in the present paper. However, Obremski & Fejer did observe in some of their experiments what appear to be intermittently growing and decaying wavelike disturbances that were precursers of turbulent bursts. In these cases, the imposed oscillation frequencies were very low compared with the disturbance frequencies. In the notation used in this paper, the values of ω_1/Ω in their experiments were about 50. A rough comparison of the low-frequency, $\omega_1/\Omega = 14$, results for plane Poiseuille flow and the very-low-frequency results of Obremski & Fejer can be made. For example, figure 5 of Obremski & Fejer

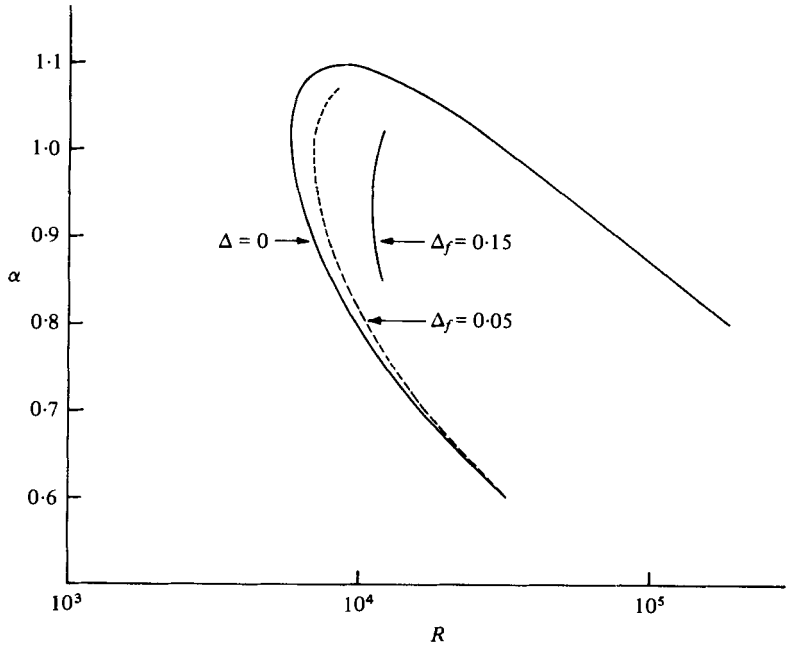

FIGURE 5. The shift of the nose of the neutral curve due to the oscillations for $\Delta_f = 0{\cdot}05$ and $0{\cdot}15$ ($\beta = 16{\cdot}1$).

shows wave-like disturbance beginning to appear slightly ahead of the minimum velocity near the edge of the basic flow. These disturbances then appear to grow and to persist as the basic velocity increases, i.e. during the early part of the acceleration of the basic state. The centre-line velocity of OPP flow is mainly proportional to $\sin \Omega t$ for large values of β ($\beta = 7{\cdot}453$ for $\omega_1/\Omega = 14$). Figure 14 shows that the instantaneous growth rate G of the disturbance becomes positive near the value of $t = 7T$ (i.e. near $t = \pi/\Omega$). Thus the large transient growth of the disturbance occurs in the time interval $\pi/\Omega < t < 2\pi/\Omega$. This is the part of the oscillation cycle in which the centre-line velocity is lower than the mean velocity. Furthermore, Obremski & Fejer report that complete transition (i.e. turbulence persisting for the entire oscillation cycle) occurs at a slightly smaller value of the mean Reynolds number than the value of transition Reynolds number of the steady flow. This behaviour is not inconsistent with the slight mean destabilization that occurs by oscillating the flow with frequency $\Omega = \omega_1/14$.

It is of interest to determine the shift of the neutral stability curve of steady plane Poiseuille flow, that results from the imposed oscillations. Such a calculation was made for a fixed value of β and for $\Lambda = \Lambda_f R_c/R$. The value of Λ_f was chosen arbitrarily. This variation of the relative oscillating pressure gradient amplitude corresponds to a constant absolute value of the oscillating pressure gradient amplitude Q_f for all Reynolds numbers R. The results of this calculation are shown in figure 5. Here the value of β is $16{\cdot}1$ corresponding to $\omega_1/\Omega = 3{\cdot}0$ at $\alpha = \alpha_c$ and $R = R_c$. This value of β was chosen because it gives the biggest change in growth rate of the principal steady-flow disturbance at the critical point. The dashed curve in figure 5 is the change in the neutral curve for $\Lambda_f = 12{\cdot}96$. This value of Λ_f corresponds to the value of $\Delta_f = 0{\cdot}05$ (recall $\Delta = \Lambda/\beta^2$). For these small values of Δ it is sufficient to calculate only the first

α	R_n	$\mathscr{R}\left(\frac{d\lambda_{(1,0)}}{dR}\right)_n \times 10^6$	$\frac{\omega_1}{\Omega}$	$\mathscr{R}(\lambda_{(1,2)})$	R_{ns}
0·6	32 293	0·228	5·548	−0·3584	32 420
0·7	16 355	0·590	4·025	−0·5384	16 640
0·8	9 882·4	1·158	3·257	−0·6564	10 370
0·9	6 965·0	1·377	2·912	−0·7360	7 693
0·95	6 207·5	1·885	2·868	−0·7792	7 101
1·0	5 815·0	1·810	2·930	−0·8764	6 959
1·0206	5 772·22	1·719	3·0	−0·8764	7 047
1·05	5 890·0	1·361	3·178	−0·9440	7 555
1·07	6 186·0	1·015	3·400	−1·0068	8 345
1·05	19 384	−0·399	8·429	0·094	19 440
1·0206	26 247	−0·338	10·37	0·8868	26 560
1·0	31 955	−0·299	11·84	1·4424	32 350
0·9	77 840	−0·142	21·11	3·6456	78 190
0·8	188 250	−0·058	36·75	4·194	188 400

TABLE 4. The values of the derivative of the steady plane-Poiseuille-flow growth rate $\lambda_{(1,0)}$ with respect to Reynolds number R, the perturbation coefficient $\mathscr{R}(\lambda_{(1,2)})$, the frequency ratio (ω_1/Ω) and the neutrally stable value of Reynolds number, R_{ns}, of the oscillatory flow with amplitude $\Delta_f = 0{\cdot}05$

perturbation term $\lambda_{(l,2)}$ in expansion (15*b*). For small values of Δ and $(R-R_n)$ one has the Taylor's expansion in two variables for α = constant,

$$\lambda_{(l)} = \lambda_{(l,0)} + \lambda_{(l,2)n}\Delta^2 + \left.\frac{d\lambda_{(l,0)}}{dR}\right|_n (R-R_n) + \ldots, \tag{37}$$

where the subscript n denotes values on the steady-flow neutral curve.

On the steady-flow neutral curve $\mathscr{R}(\lambda_{(1,0)}) = 0$ and on the unsteady-flow neutral curve $\mathscr{R}(\lambda_{(1)}) = 0$. Hence, by evaluating equation (37) on the unsteady-flow neutral curve one obtains

$$R_{ns} \simeq \left(1 - \mathscr{R}(\lambda_{(1,2)n})\,\Delta^2 \Big/ \mathscr{R}\left(\left.\frac{d\lambda_{(1,0)}}{dR}\right|_n\right) R_n\right) R_n. \tag{38}$$

This formula was used to compute points on the dashed curve in figure 5. Table 4 gives the values of $\mathscr{R}(d\lambda_{(1,0)}/dR)_n$ and $\mathscr{R}(\lambda_{(1,2)})_n$ that were used to compute the dashed curve. The values of $\mathscr{R}(d\lambda_{(1,0)}/dR)_n$ were computed by using five-point central difference formulae. These values are believed to be accurate to the number of figures shown in the table 4.

The inner solid curve in figure 5 is the nose of the neutral curve of OPP flow with $\Delta_f = 0{\cdot}15$ ($\Lambda_f = 38{\cdot}88$ at $\alpha = \alpha_c$, $R = R_c$) and $\beta = 16{\cdot}1$. Note that the critical Reynolds number is nearly doubled.

The results shown in figure 5 indicate that at the apparent optimum stabilizing frequency, $\beta = 16{\cdot}1$, plane Poiseuille flow can be moderately stabilized by small-amplitude oscillations and substantially stabilized by moderately-large-amplitude oscillations. However, the stabilization achieved in figure 5 requires very large values of the relative oscillating pressure gradient amplitude. In an actual experiment in which a liquid such as water is the working medium it would seem very difficult to impose such large oscillating pressure gradients.

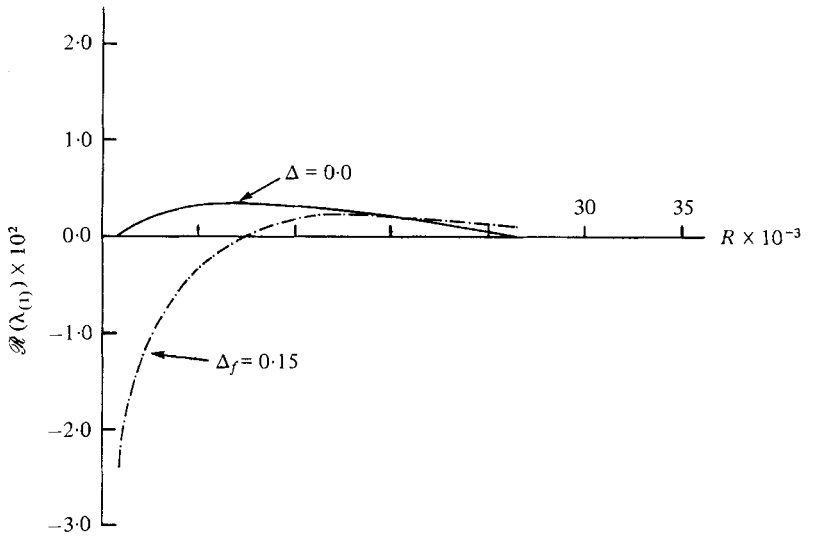

FIGURE 6. The growth rate $\mathscr{R}(\lambda_{(1)})$ of the principal disturbance mode as a function of Reynolds number R for fixed values of (dimensional) oscillatory pressure-gradient amplitude ($\Delta_f = 0{\cdot}15$) at $\alpha = 1{\cdot}0206$, $\beta = 16{\cdot}1$.

R	ω_1/Ω	$\mathscr{R}(\lambda_{(1,2)})$	$\mathscr{R}(\lambda_{(1,4)})$
5772·22	3·0	−0·8763	−7·915
8000	3·93	−0·9648	−2·632
11000	5·10	−0·9096	17·4496
15000	6·58	−0·6364	46·053
20000	8·32	−0·0704	32·104
26247	10·37	0·8868	−154·35

TABLE 5. Values of $\mathscr{R}(\lambda_{(1,2)})$ and $\mathscr{R}(\lambda_{(1,4)})$ for fixed frequency oscillation $\beta = 16{\cdot}1$ and $\alpha = \alpha_c = 1{\cdot}0206$ for various values of Reynolds number in the unstable region of the steady basic flow

Figure 6 shows the graphs of $\mathscr{R}(\lambda_{(1)})$ versus Reynolds number in the unstable region of plane Poiseuille flow for $\beta = 16{\cdot}1$, $\alpha = \alpha_c = 1{\cdot}0206$ and for two values of Δ; $\Delta = 0$ and $\Delta_f = 0{\cdot}15$. The values of $\mathscr{R}(\lambda_{(1,2)})$ and $\mathscr{R}(\lambda_{(1,4)})$ for cases depicted in figure 6 are given in table 5, but the graph of $\mathscr{R}(\lambda_{(1)})$ for $\Delta_f = 0{\cdot}15$ was computed using $M = 40$ terms of the series (15) and the Shanks transformation. It is interesting to note, in this case, that the flow is destabilized on the back of the neutral curve of the steady flow.

Finally, figure 7 shows the graphs of the values of $\mathscr{R}(\lambda_{(1)})$ as a function of the velocity amplitude ratio Δ for various values of R and α and for $\beta = 16{\cdot}1$ ($\omega_1/\Omega = 3$ at $\alpha = \alpha_c$ and $R = R_c$). The graphs of $\mathscr{R}(\lambda_{(1)})$ were computed using $M = 40$ terms in the expansion (15) and the Shanks transformations. These graphs were drawn up to the values of Δ at which the Shanks table seemed to converge to about three significant figures.

It is interesting to note that, at higher values of Reynolds number, the series (15*b*) has a very small radius of convergence and that the Shanks transformation (or any other sequence transformation in the Vanden-Broeck & Schwartz 1979 scheme) did not produce converged values of $\lambda_{(l)}$ for much larger values of Δ. For example, the

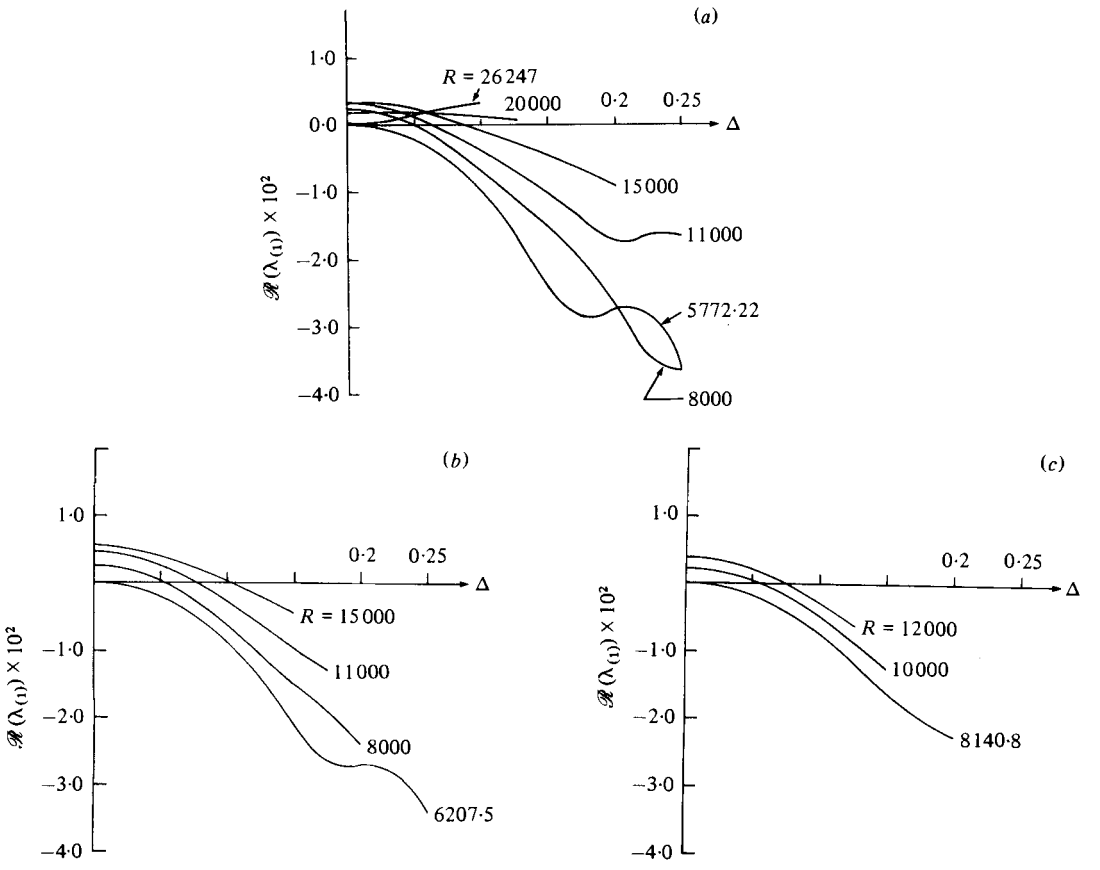

FIGURE 7. The growth rates $\mathscr{R}(\lambda_{(1)})$ versus Δ at $\beta = 16{\cdot}1$ and for various values of R. (*a*) for $\alpha = 1{\cdot}0206$, (*b*) for $\alpha = 0{\cdot}95$, (*c*) for $\alpha = 0{\cdot}85$.

case of $R = 26247$ in figure 7(*a*) has a radius of convergence of $\Delta_0 = 0{\cdot}05$ and the Shanks transformation yields converged values of $\mathscr{R}(\lambda_{(1)})$ up to $\Delta = 0{\cdot}1$. The graphs of figure 7 were used to interpolate the values of R that give neutral stability, $\mathscr{R}(\lambda_{(1)}) = 0$ at $\alpha = 1{\cdot}0206$, $0{\cdot}95$ and $0{\cdot}85$ and $\Delta_f = 0{\cdot}15$ (where $\Delta = \Delta_f R_c/R$ at $\alpha = \alpha_c$), and from which the neutral curve for $\Delta_f = 0{\cdot}15$ in figure 5 was constructed.

5. Concluding remarks

It has been shown that the sinusoidally oscillating plane Poiseuille flow is more stable than the steady plane Poiseuille flow for a wide range of frequencies of the imposed oscillation and for substantial values of oscillation amplitude. The range of imposed oscillation frequencies which stabilizes the flow in the vicinity of the steady-flow neutral point $\alpha = \alpha_c = 1{\cdot}0206$, $R = R_c = 5772{\cdot}22$ ranges from the very high value of $\Omega = 8\omega_1$ to the fairly low value of $\Omega = \omega_1/10$. For even lower values of frequency, $\Omega < \omega_1/10$ the oscillatory flow is slightly less stable than the steady flow. The range of oscillation amplitudes for which this situation holds seems to be as high as $\Delta = 0{\cdot}25$. The optimal value of imposed frequency Ω for stabilizing plane Poiseuille flow seems to be about $\Omega = \omega_1/3$ at $\alpha = \alpha_c$, $R = R_c$. At this value of Ω $\beta = 16{\cdot}1$. For

$\beta = 16{\cdot}1$ and $\Delta_f = 0{\cdot}15$ one can achieve a doubling of the critical value of the Reynolds number. At the values of Reynolds number corresponding to the back of the steady flow neutral curve the oscillatory flow is slightly *less* stable than the steady flow.

It was found that in every case that was examined (about 20 combinations of values of α, R and β) only the principal disturbance mode of the steady flow was significantly altered by the imposed oscillations even for values of Δ as large as 0·25. This is contrary to the results of Grosch & Salwen (1968) who found, numerically, that at $\alpha = \alpha_c$, $R = R_c$, $\Omega = \omega_1$ and $\Delta = 0{\cdot}105$ the oscillations caused a drastic destabilization of one of the higher modes.

The results obtained in this investigation differ considerably from those of Grosch & Salwen. Not only has the destabilization found by Grosch & Salwen not been confirmed, but also the degree of stabilization for very small values of Δ that was presented by them differs substantially from the values found in the present investigation. Figure 11 of the paper by Grosch & Salwen presents the graph of $\mathscr{R}(\lambda_{(1)})$ versus Λ for $\omega_1/\Omega = 1$, $\alpha \simeq \alpha_c$ and $R \simeq R_c$ (using the notation of the present paper). From this graph one can estimate the value of $\mathscr{R}(\lambda_{(1,2)})$ that results from Grosch & Salwen's calculations. Their value of $\mathscr{R}(\lambda_{(1,2)})$ turns out to be about -2×10^2 which is about three orders of magnitude greater than the value obtained in the present investigation (see table 2). Such a large value for $\mathscr{R}(\lambda_{(1,2)})$ seems rather unlikely in view of the thinness of the oscillation-induced Stokes layer when $\omega_1/\Omega = 1$ (i.e. $\beta \approx 28$). The stability characteristics of OPP flow at very high frequencies (see table 3) are in qualitative agreement with Hall's results.

The calculations performed in this investigation were based on solving the system of time periodic stability equations by series expansions in the amplitude parameter Δ. As many as 40 terms of this series were computed and nonlinear sequence transformations of the partial sums were used to evaluate the series well past its radius of convergence. This method of solving the stability equations, in contrast to direct numerical time integration of the equations (see Grosch & Salwen 1968) is very efficient. Also, one obtains an analytical result in terms of the amplitude Δ for fixed values of the other parameters.

It seems that the range of values of Δ for which accurate values of $\lambda_{(l)}$ can be obtained with as many as 40 terms of series (15) is disappointingly limited. However, one must realize that in the range of oscillation frequency considered here a value of Δ equal to 0·1 corresponds to very large values of the oscillatory pressure gradient compared to the steady flow pressure gradient. Hence, the range of values of Δ between 0·0 and 0·25 would seem to cover the important range for high Reynolds number.

Probably the greatest advantage offered by the perturbation method of computing the Floquet exponents as compared to numerical time integration is that the perturbation method allows the calculation of the effects of the imposed oscillations on each individual disturbance mode of the steady flow. Hence, this method provides a means of making a more detailed analysis of the change of the stability characteristics that are induced in the basic flow by the imposed oscillations.

A comparison of computer times required by the perturbation and time integration methods may be of interest. On the DEC-10 computer system using double-precision arithmetic about 2·5 min of CPU time is required to compute 40 terms of the series expansion (15) for the system of $N = 26$ equations (12). The computational time required to compute the 40 terms of the perturbation series depends only on the

value of N, not the values of α, R or β and increases like N^2. The numerical time integration of equations (12) is very sensitive to the value of ω_1/Ω (i.e. β). For very low values of the frequency Ω one must use many time steps in order properly to resolve the steady flow frequencies such as ω_1. Furthermore, one must either integrate system (12) for the entire fundamental matrix over one period of the imposed oscillations, or one must integrate system (12) over several periods (at least three of them) for a single vector solution. In the first case, the amount of computation is proportional to KN^3, in the second case the amount of computation is proportional to PKN^2, where K is the number of time steps and P is the number of complete imposed oscillation periods over which the time integration is executed. For the cases that were numerically integrated in this investigation, only the second method was used. In the higher-frequency cases, $\omega_1/\Omega = 3$ of figure 1, the time integration required 1·5 min of CPU time per period. Hence, for three periods, 4·5 min of CPU time was required. For the low-frequency case, $\omega_1/\Omega = 14$ of figures 4 and 5, about 8 min of CPU time per period was required. In this case, 1400 equal time steps per period were required to obtain accurate results for the change in ϵ between the beginning and end of a period. These results can be used to infer the CPU time requirements for the calculation of the fundamental matrix and it is clear that such a calculation is comparatively very expensive. The price one has to pay to gain this computational advantage of the perturbation method is its limited range of validity in the variable Δ although this range may be increased by a more careful analysis of the series coefficients. Also, the programming effort required for the series expansion method was substantial compared to the programming effort of the time integration method.

This research was supported by the National Science Foundation under Grant no. CME-7900929. A portion of the computational expenses was provided by the Catholic University of America. The author is appreciative of this support.

REFERENCES

Davis, S. H. 1976 The stability of time-periodic flows. *Ann. Rev. Fluid Mech.* **8**, 57–74.

Coddington, E. A. & Levinson, N. 1955 *Theory of Ordinary Differential Equations*, pp. 78–81. McGraw-Hill.

Finucane, R. G. & Kelly, R. E. 1976 Onset of instability in a fluid layer heated sinusoidally from below. *Int. J. Heat Mass Transfer* **19**, 71–85.

Gaunt, D. S. & Guttmann, A. T. 1974 Asymptotic analysis of coefficients. In *Phase Transitions and Critical Points* (ed. C. Domb & M. S. Green), vol. 3, pp. 181–243. Academic.

Gottlieb, D. & Orszag, S. A. 1978 *Numerical Analysis of Spectral Methods: Theory and Applications*, pp. 143–148. Soc. for Industrial and Appl. Math.

Grosch, C. E. & Salwen, H. 1968 The stability of steady and time-dependent plane Poisueille flow. *J. Fluid Mech.* **34**, 177–205.

Hall, P. 1975 The stability of Poiseuille flow modulated at high frequencies. *Proc. R. Soc. Lond.* A **344**, 453–464.

Herbert, D. M. 1972 The energy balance in modulated plane Poiseuille flow. *J. Fluid Mech.* **56**, 73–80.

Kerczek, C. von & Davis, S. H. 1974 Linear stability theory of oscillatory Stokes layers. *J. Fluid Mech.* **62**, 689–703.

Miller, J. A. & Fejer, A. A. 1964 Transition phenomena in oscillating boundary layer flows. *J. Fluid Mech.* **18**, 438–448.

OBREMSKI, H. J. & FIEJER, A. A. 1967 Transition in oscillating boundary layer flows. J. Fluid Mech. 29, 933111.

ORSZAG, S. A. 1971 Accurate solution of the Orr-Sommerfeld stability equation. J. Fluid Mech. 50, 689–703.

ROSENBLAT, S. & HERBERT, D. M. 1970 Low-frequency modulation of thermal instability. J. Fluid Mech. 43, 385-398.

SHANKS, D. 1955 Non-linear transformation of divergent and slowly convergent sequences. J. Math. & Phys. 34, I-42.

VANDEN-BROECK, J. M. & SCHWARTZ, L. W. 1979 A one-parameter family of sequence transformations. SIAM J. Math. Anal. 10, 658-666.

VAN DYKE, M. 1974 Analysis and improvement of perturbation series. Quart. J. Mech. Appl. Math. 27, 423-450.

YAKUBOVICH, V. A. & STARZHINSKII, V. M. 1975 Linear differential equations with periodic coefficients (transl. D. Louvish), cha. 4. Wiley.